

LG

## Transient Behavior of Point Defect in CZ Silicon Crystals

Kwang Hun Kim, Il Soo Choi, Jong Hoe Wang, Hong Woo Lee  
Crystal Growth Research Team, R & D Center, LG Siltron Inc., Korea

### 1. Introduction

The behavior of point defects in a Czochralski(CZ)-grown silicon crystal has been studied by many authors because the point defect cluster was one of the hot issues in semiconductor technology for last decade. For high quality silicon crystals we need to control the intrinsic point defects in silicon single crystal. It is well known that the concentration of intrinsic point defects in the Czochralski growth of silicon single crystals is a function of the crystal pull rate  $V$  and the axial temperature gradient  $G$  at the melt/crystal interface inside the crystal [1- 2].

In this paper, we have optimized the parameters  $\mu_1$  and  $\mu_2$  which control the radial and axial temperature distributions in the silicon crystal. And transient point defect numerical analysis has been performed for the growth halt experiment with the 150mm silicon single crystals to study the macroscopic behavior of point defect. It has been demonstrated that predicted point defect distributions are in good qualitative agreement with experimental results.

### 2. Mathematical Model

The mathematical model equations to predict the time dependent point defect concentrations were developed and shown in this section. The modelled temperature distributions in the crystal phase were used as an input for the calculation of concentrations and thermophysical properties of intrinsic point defects - vacancy and (self-) interstitial.

#### 2.1 Modelled Temperature Distributions

According to Wang et. al[3-4], the temperature distributions in the crystal phase is given as

$$T(r, z) = \exp(-\mu_1 (r/R)^2 z) \left[ T_a + (T_m - T_a) \frac{\exp(\mu_2 (z_{top} - z))}{\exp(\mu_2 - z)} \right] \quad (1)$$

$$z_{top}(t) = z_{top}(0) + \int_0^t V(\tau) d\tau \quad (2)$$

which contains three parameters ( $\mu_1, \mu_2, T_a$ ) and one process condition. The parameters  $\mu_1$  and  $\mu_2$  control the radial and axial temperature distributions, respectively.  $T_a$  is approximately equal to the temperature at the top surface of the silicon single crystal. We performed calculations with the optimized parameter values  $\mu_1, \mu_2$  and  $T_a = 1000\text{K}$ .

$R, T_m, V$  and  $z_{top}$  are the radius of growing crystal, the melting temperature of silicon, the crystal pulling rate and the height of the crystal, respectively.

#### 2.2 Transient Point Defect Dynamics

Transient conservation equations for the transient change, convection, diffusion and recombination of intrinsic point defects are written in terms of concentration of interstitial and vacancy as

$$\frac{\partial C_I}{\partial t} + V \frac{\partial C_I}{\partial z} = \nabla \cdot (D_I \nabla C_I) + k_{IV} (C_I^{eq} C_V^{eq} - C_I C_V) \quad (3)$$

$$\frac{\partial C_V}{\partial t} + V \frac{\partial C_V}{\partial z} = \nabla \cdot (D_V \nabla C_V) + k_{IV} (C_I^{eq} C_V^{eq} - C_I C_V) \quad (4)$$

$C_I$  and  $C_V$  are interstitial and vacancy concentrations computed inside the growing crystal by solving field equations on the basis of modelled temperature.  $C_I^{eq}$  and  $C_V^{eq}$  are the equilibrium concentrations of interstitials and vacancies, respectively, at the local temperature  $T$  of the crystal.  $D_I$  and  $D_V$  are the diffusion coefficients, and  $k_{IV}$  is the kinetic rate constant for the rate of recombination of interstitials and vacancies. The cylindrical co-ordinate system  $(r, z)$  is centered at the center of the melt/crystal interface. The continuum description of point defect dynamics is completed by supplying expressions for the equilibrium, transport and kinetic parameters.

The solutions of the transient second order partial differential equations require the initial and boundary conditions. The steady state solutions are used for the initial condition. We assume that the interstitial and vacancy concentrations are in equilibrium at the melt/crystal interface. The axis of the crystal ( $r = 0$ ) is taken as an axis of symmetry. We also assume that the flux of point defect is zero along the exposed crystal surface. Additional calculations with equilibrium condition along all exposed crystal surface were performed to study the influence of boundary conditions on the point defect distributions. Other boundary conditions are possible.

A thermophysical parameter set of point defects obtained by Wang et al. [5, 6] is used for the transient point defect dynamic analysis. In this analysis, the enthalpies of formation of the point defects are assumed to be zero. The comparison of steady-state point defect dynamic analysis and experimental results for OiSF-ring diameter with slow change of crystal pull rate has been discussed in detail in ref. [6].

### **3. Numerical Method**

The Galerkin finite element method is used for the discretization of complete set of the mathematical model. The intrinsic point defect concentration fields are represented in expansions of Lagrangian biquadratic basis functions. A mesh is formed of quadrilateral elements which span the computational domains corresponding to the crystal phase. The field equations are put into the weak form, and boundary conditions are imposed in the normal manner [7, 8].

Implicit Euler method is used for the time-dependent calculations. In the continuum balance equations for the transport and interactions of intrinsic point defects without accounting for the formation of aggregates, the crystal height is changed throughout the Czochralski process. In evaluating the time derivatives,  $\partial C_I / \partial t$  and  $\partial C_V / \partial t$ , we use the procedure developed by Lynch and Gray [9] to consider the mesh deformation due to the change of crystal height. The detailed numerical methods used in this work are described in ref. [5] and this approach has proven to be both accurate and robust in a variety of calculations.

## **4. Results and Discussion**

### **4.1 Optimization of $\mu_1$ and $\mu_2$**

The thermophysical parameters were selected to minimize the difference between the results of defect dynamic analysis and the experimental measurements and to predict quantitatively  $R_{\text{OiSF}}$  for a given hot zone configuration. Although there is no rigorous method to estimate the optimum parameter set which enables to minimize the difference between the results of defect dynamic analysis and the experimental measurements, the objective function is used to quantify the goodness of fitting the thermophysical properties to experimental data. The objective function( ) is as follows

$$\frac{1}{n} \sqrt{\sum_{i=1}^n [R_{\text{OisF}}^{\text{predicted}}(V_i) - R_{\text{OisF}}^{\text{experiment}}(V_i)]^2} \quad (5)$$

where  $\{V_i\}$  is a set of crystal pull rates within a range for which R-OiSF is observed experimentally. Table.1 shows the change of objective function( ) for  $\mu_1$  and  $\mu_2$ . Therefore the optimized  $\mu_1$  and  $\mu_2$  are 0.014 and 0.062, respectively.

#### 4.2 Growth Halt Experiment

In this work, crystals were grown with a crystal pull rate of  $V_{\text{high}}$ , until steady state has been reached. Then the crystal pull rate was decreased abruptly to  $V_{\text{low}}$  near to zero. Then the crystal growth was held at the ingot position of 60cm for various growth-halt time(30, 60, 120, 180 minutes)[4, 10]. And then the crystal pull rate was increased again to  $V_{\text{high}}$ . Fig. 1 shows the crystal pulling rate near the growth halt position. Fig. 2 shows the X-ray topography of a vertical section of 150mm silicon single crystal for (a) 30 min and (b) 180 min, growth halt experiment. It is clearly observed that the defect features are not limited to the slowly grown crystal part, but spread into the regions of higher crystal pull rate, which would be completely vacancy-rich under steady state conditions. In this work, the experimental results are well in agreement with the transient point defect dynamic analysis. The transient point defect dynamics analysis is a useful tool to predict point defect distributions with changes in operating conditions, such as the crystal pull rate.

#### 5. Conclusions

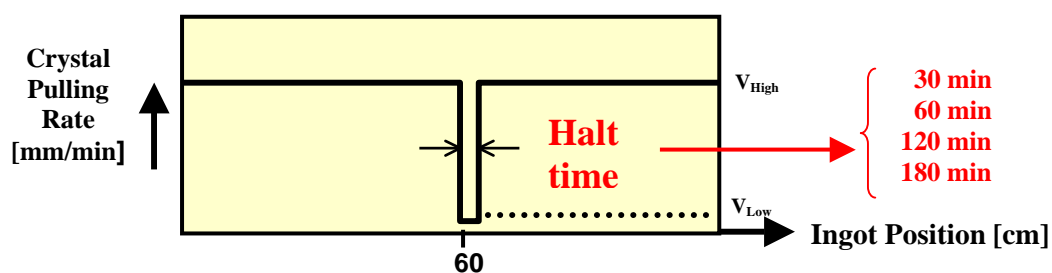
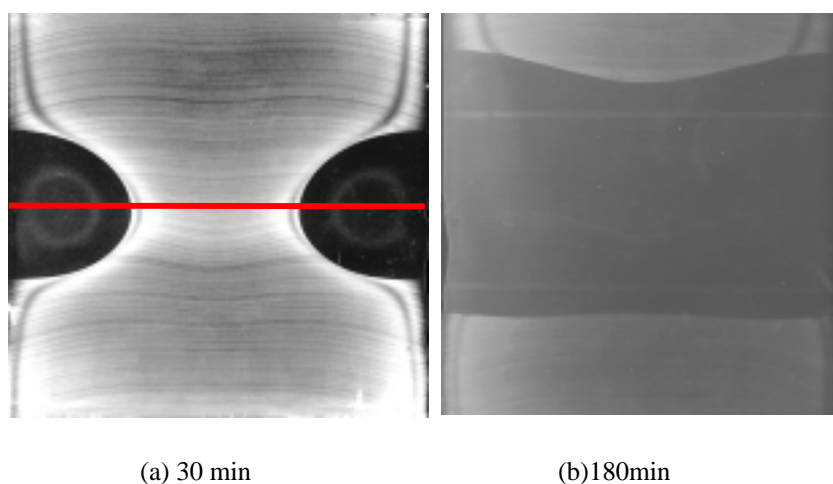
We have optimized the parameters  $\mu_1$  and  $\mu_2$  which control the radial and axial temperature distributions in the silicon crystal to minimize the difference between the results of defect dynamic analysis and the experimental measurements and predict quantitatively  $R_{\text{OisF}}$  for a given hot zone configuration. In this study, we have performed numerical calculations based on the transient mathematical model which has been developed to describe the intrinsic point defect distribution in Czochralski-grown 150mm silicon single crystals of the growth halt experiment. It has been demonstrated that the predicted point defect distributions are in good qualitative agreement with the experimental results.

#### REFERENCES

- [1] Voronkov, V.V. : J. Crystal Growth 59 625(1982).
- [2] Voronkov, V.V. and Falster, R. : J. Crystal Growth 194 76(1998).
- [3] Wang, J.H., Oh, H.J., Park, B.M., Lee, H.W. and Yoo, H.D. : The 13th American Conference of Crystal Growth and Epitaxy, Burlington, Vermont, USA, Aug. 12-16 (2001).
- [4] Wang, J.H., Oh, H.J., Park, B.M., Lee, H.W. and Yoo, H.D. : J. Korean Ass. Crystal Growth 11 259(2001).
- [5] Wang, J.H., Oh, H.J. and Yoo, H.D. : Korean J. Chem. Eng. 18 81(2001).
- [6] Oh, H.J., Wang, J.H. and Yoo, H.D. : J. Korean Ass. Crystal Growth 10 356(2000).
- [7] Wang, J.H., Kim, D.H. and Chung, D.S. : Korean J. Chem. Eng. 13 503(1996).
- [8] Wang, J.H., Kim, D.H. and Yoo, H.D. : J. Crystal Growth 198/199 120(1999).
- [9] Lynch, D.R. and Gray, W.G. : J. Comput. Phys. 36 135(1980).
- [10] Park, B.M. and Choi, I.S. : The 48th Spring Meeting of the Japan Society of Applied Physics and Related Societies, Tokyo, Japan, Mar. 28-31 (2001).

**Table.1. The change of objective function for  $\mu_1$  and  $\mu_2$** 

$\mu_2 \backslash \mu_1$	0.01	0.013	0.014	0.015	0.016	0.017	0.018	0.02	0.03	0.04
0.06	5.68	3.05	2.52	2.27	2.31	2.55	2.90	3.70	7.29	9.72
0.061	5.02	2.77	2.32	2.26	2.47	2.81	3.19	4.05	7.64	10.03
0.062	4.44	2.54	2.25	2.39	2.71	3.11	3.56	4.43	8.01	10.34
0.063	3.92	2.33	2.35	2.64	3.04	3.50	3.96	4.86	8.37	10.65
0.064	3.46	2.36	2.60	2.99	3.46	3.94	4.41	5.31	8.78	11.00
0.065	3.10	2.60	2.98	3.44	3.94	4.42	4.90	5.80	9.18	11.35
0.066	2.91	3.00	3.47	3.97	4.47	4.96	5.44	6.32	9.62	11.71
0.067	2.92	3.54	4.04	4.55	5.06	5.54	6.01	6.87	10.06	12.10
0.068	3.19	4.18	4.70	5.21	5.70	6.17	6.62	7.45	10.53	12.49
0.069	3.71	4.91	5.43	5.92	6.40	6.85	7.29	8.09	11.04	12.93
0.07	4.46	5.75	6.25	6.72	7.18	7.60	8.02	8.77	11.57	13.37

**Fig.1. Crystal pulling rate near the growth halt position. Crystal pulling rate was dropped abruptly from  $V_{High}$  to  $V_{Low}$** **Fig.2. X-ray topograph of an axial section of CZ single crystal silicon grown at lower crystal pulling rate for (a) 30 min and (b) 180 min. The diameter of CZ grown silicon crystal is 150 mm.**